

INTERNATIONAL SOCIETY FOR SOIL MECHANICS AND GEOTECHNICAL ENGINEERING



This paper was downloaded from the Online Library of the International Society for Soil Mechanics and Geotechnical Engineering (ISSMGE). The library is available here:

<https://www.issmge.org/publications/online-library>

This is an open-access database that archives thousands of papers published under the Auspices of the ISSMGE and maintained by the Innovation and Development Committee of ISSMGE.

Mechanical analysis of soil arching under dynamic loads

Han Gaoxiao, Gong Quanmei, Zhou Shunhua
*Key Laboratory of Road and Traffic Engineering of Ministry of Education,
Tongji University, Shanghai, China*



ABSTRACT

Soil arching is a common phenomenon in pile supported geosynthetic-reinforced or unreinforced embankments resting on soft soil. Due to soil arching, stress acting on soft soil or geosynthetic reinforcement decreases and stress on piles increases, this can reduce the settlement difference along the subgrade cross-section. Now most of the high-speed railway subgrades in soft soil area in China have been designed considering of the action of soil arching. But during the period of service life of the railway line, the subgrade will carry on high-cycle dynamic loads and when the subgrade is not high enough, the soil arching maybe influenced and the permanent deformation will increase. In this paper the properties of soil arching under dynamic loads have been investigated by performing numerical studies using the Discrete Element Method (DEM) and model experiments. In the numerical study, soil was modeled as particles using the linear contact stiffness model. The influence of the covering soil thickness and the dynamic loads amplitude were proposed in this paper.

RÉSUMÉ

L'effet de voûte est un phénomène courant dans la réalisation du terrassement type pieux de fondation ou type pieux et géotextile sur le sol compressible. Par son existence, la contrainte sur le sol compressible ou sur le matériel de renforcement est diminuée tandis que celle sur les pieux, augmentée, ce qui fait diminuer ainsi le tassement différentiel à la section transversale du terrassement. Actuellement, le Design en Chine tient en compte de l'effet de voûte pour la plupart de construction de terrassement TGV sur le sol compressible. Mais pour la ligne TGV pendant son exploitation, la déformation résiduelle du terrassement augmentera aussi sous l'action des charges dynamique de cycle lorsque ce terrassement a une hauteur relativement basse. Le présent texte présente une étude, menée avec la méthode DEM et le Model-Based Testing, sur la répartition des charges sous l'effet de voûte, son mode destructif, ainsi que l'impact de l'épaisseur du remblai et de l'amplitude des charges dynamiques sur l'effet de voûte.

1 INTRODUCTION

Piled embankments are increasingly used to construct high-speed railway and highway on soft soils due to small total and differential settlements compared to the traditional soft soils improvement methods. The interactions among embankment fill, geosynthetic reinforcement, pile (cap) and foundation soil are complex. Since compression stiffness of the pile is greater than that of the foundation soil, the embankment fill mass directly above the foundation soil has a tendency to move downward. This movement is partially restrained by shear stress from the embankment fill mass directly above the pile cap. The shear stress increases the pressure acting on the pile cap but reduces the pressure on the foundation soil. This load transfer mechanism was termed the "soil arching effect" by Terzaghi (1943). The inclusion of geosynthetic reinforcements complicates the load transfer mechanism. The soil arching has a significant influence on the behavior of piled embankments.

Consequently, in order to get thorough understandings of soil arching mechanism within piled embankments a number of research studies associated with this subject have been performed in the past two decades. Hewlett and Randolph (1988) conducted 3D

model tests and presented a semi-spherical model to describe soil arching. Low et al. (1994) undertook 2D model tests to evaluate soil arching. However, pile - subsoil relative displacement was not taken into account. Han and Gabr (2002) conducted a numerical analysis on geosynthetic-reinforced and pile-supported earth platform over soft soil and studied the effects of pile material elastic modulus and geosynthetic stiffness on the degree of soil arching. They observed that the soil arching in the embankment soil was increased with an increase in the height of embankment fill and elastic modulus of the pile material. However, soil arching was decreased as the tensile stiffness of geosynthetic reinforcement was increased. Based on 2-D physical and numerical modeling of pile-supported earth platform over soft soil, Jenck et al. (2007) observed that the load transfer onto piles due to soil arching was effectively controlled by shearing mechanisms (development of shearing in the granular fill due to differential settlements at the platform base between the soft soil and the rigid piles, leading to arching which partially transfers the loads onto the piles) and shear strength of the platform or embankment material. Chen Yun-min et al. (2008) conducted experimental investigation on reinforced and unreinforced piled embankments to study the effects of pile - subsoil relative displacement, embankment height, cap beam

2.4 Model Test Procedure

After installation of the test set-up, sand was filled one layer after another and compacted, during which soil stress transducers (SSTs) were placed at certain depth and the variation of stress would be recorded. There were six transducers in the test. The number of transducers were SST1-6 (As showed in Figure 1).After reached required height of sand opened the hole which was closed before to form a soil arching under self weight. Then, for Test1, the cylinder was removed and the sand was divided into two parts to investigate the formed soil arching (As showed in Figure 4). For the rest of the test, the value of transducers were reset to zero at first, then a dynamic load generated by the exciter and located in the center of the top of sand was applied on within a area with a diameter of 200 mm until the soil collapsing, the magnitude and frequency of the dynamic load were 140N and 50 Hz. During the process the stress was also recorded.

2.5 Test Results

2.5.1 Soil Arching under Self Weight

After the hole was opened, the stress value of SST-1、SST-3 decreased dramatically while the stress value of SST-2、SST-4、SST-5、SST-6 did not(As showed in Figure 3). So it could be considered that the height of top of soil arching was about 200mm, according to theory having been proposed and test results, the thickness of foot of soil arching could be considered to be 60mm. Moreover an approximately circular arching could be found above the hole after sand was divided into two parts and the height of the arch was 60mm. Consequently, the shape of soil arching could be determined according to the above results (Depicted as a dashed line in Figure 4). The lower bound of soil arching was a approximately circular arch which radius was 50mm and the upper bound was an elliptic arch which major axis was 200mm and minor axis 110mm.

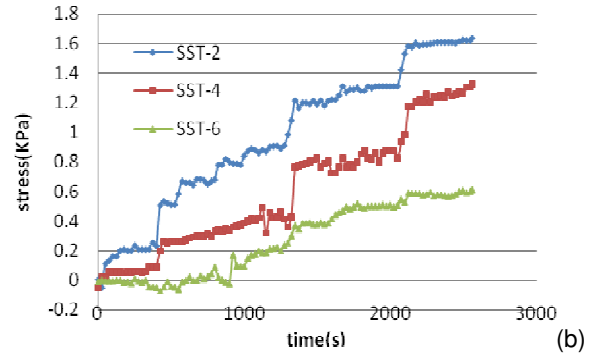
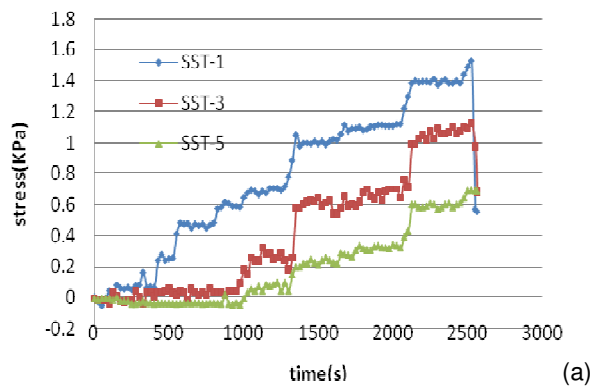


Figure 3. Variation of stress during the process of arching formed (Test 1)

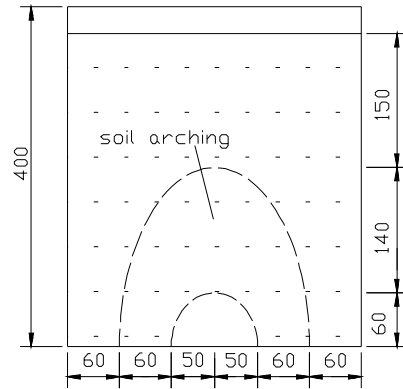


Figure 4. Soil arching under self weight unit: (mm)

2.5.2 Dynamic Stresses in the Sand

The soil arching in Test 2-4 collapsed under dynamic load and the variation of dynamic stresses showed nearly identical characteristics in Test 2-4, and only the results of Test 4 are presented herein(Figure 5). As showed in Figure 5, after the dynamic load was applied on, the dynamic stress measured by SST1、3、5 remained at stable values for a short time at first and then began to decrease to zero. The dynamic stresses measured by SST2、4、6 increased and reached a maximum value then decreased gradually to zero. The higher the SST, the longer the time required for the stress to be zero was. It could be considered that the failure of soil arching occurred at arching foot firstly and then spread upward. Although the variation of dynamic stresses was identical in Test 2-4, the required time of soil arching failure increased with the increment of sand height, from 212 seconds to 835 seconds. For Test 5, the soil arching was not failure after 200 thousand cycles of load, the dynamic stress measured by SST1、2、3、4、5、6 showed nearly identical characteristics, and only the results of SST3、4 are presented herein(Figure 6). As showed in Figure 6, the dynamic stress increased and reached a maximum value then remained at stable values. Compared Test 2、3、4 to test 5, there may be a threshold dynamic stress, when the dynamic stress

above it, the soil arching will be failure, by contrary, the soil arching will not be failure.

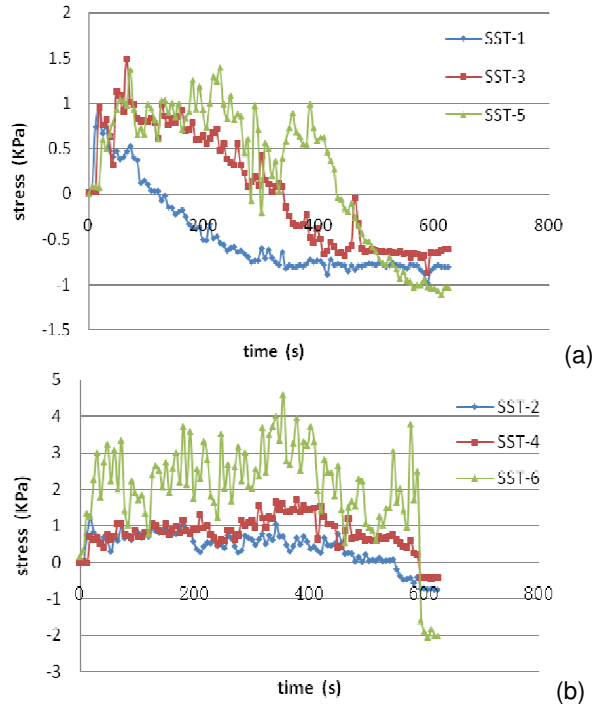


Figure 5. Variation of dynamic stress under dynamic load(Test 4)

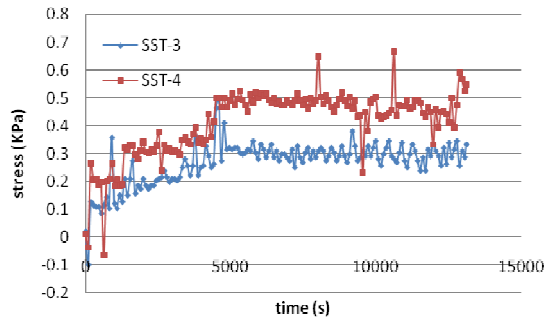


Figure 6. Variation of dynamic stress under dynamic load(Test 5)

3 PFC2D ANALYSIS OF SOIL ARCHING

3.1 Pfc2d Model

In numerical analysis, a 400 mm high and 400 mm long rectangular box was created using six walls among which there were three walls making up of the bottom of the box. And a wall, in the center of the bottom, with length of 50 mm could be removed after the box was filled with particles and achieved the initial stress condition in order to form a soil arch. A plate was created at the top of the assembly by bonding particles via contact bonds (As showed in Figure 7). After soil arching was formed a vertical load was applied on the plate. Forty six

measurement circles were installed in the model as shown in figure 10 to measure the stresses during the process of computing.

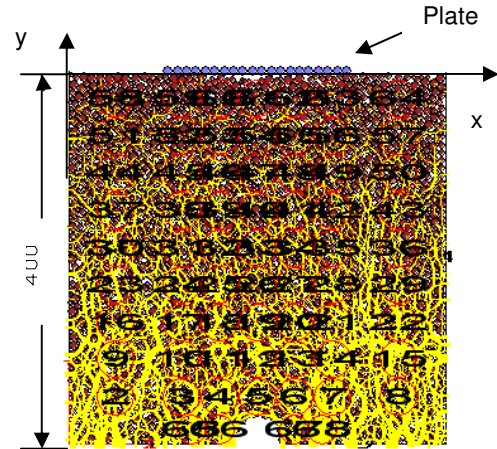


Figure 7. Numerical analysis model

The model contains about 5,000 circular particles. The microscopic properties of materials are usually calibrated or determined using known macroscopic responses. Numerical biaxial tests and shear tests are commonly used to evaluate the microscopic properties of geo-materials. In this study, biaxial tests were used to determine the micro-properties of sand to have similar mechanical properties to the sand used in former tests. The biaxial sample, used to determine the micro-mechanical parameters of sand, had a width of 0.24 m and height of 0.48 m. The particles of 2 to 10 mm in diameter were used for this determination using the biaxial test. The medium dense particle assembly was created by setting porosity (n) of 0.16. The density of particle is 2600kg/m^3 , shear stiffness and normal stiffness is both $2 \times 10^6\text{N/m}$, the coefficient of friction is 1. The above parameters were used to perform the biaxial test as outlined in PFC2D manual (Itasca, 2004). The deviatoric stress ($\sigma_1 - \sigma_2$) versus axial strain is shown in Figure 8. This plot was obtained at three confining pressures: 7.5, 15, and 30 kPa. According to the test results, Mohr's circles at failure can be plotted as shown in Figure 9. The values of c and ϕ are obtained, they are 8.96KPa and 33° respectively and very similar to the values of former test.

The computation program is detailed in Table 2. They were performed for the distribution of dynamic stress under dynamic load and the variation of dynamic stress with increment of dynamic load.

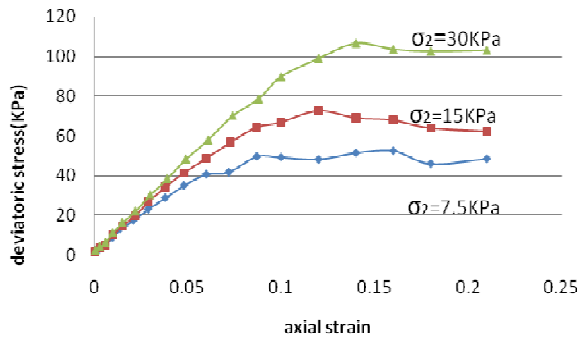


Figure 8. Deviatoric stress versus axial strain

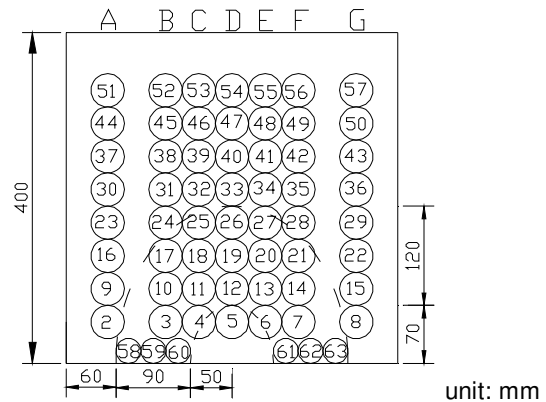


Figure 10. Soil arching in the model

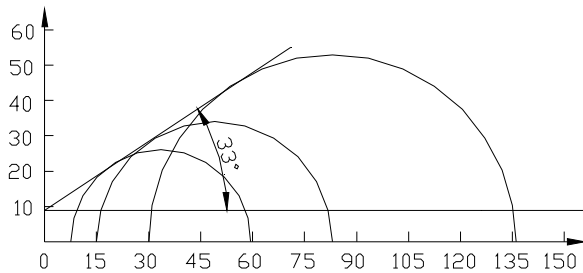


Figure 9. Mohr's circles

Table 2. Computation details

Computation No.	Load(KN)
1	$0.6+0.3\sin 20\pi t$
2	$0.6+0.2\sin 20\pi t$
3	$0.6+0.1\sin 20\pi t$

3.2 Result

3.2.1 Shape of Soil Arching

The stresses both before and after soil arching formed were compared. It could be found that stresses measured by measurement circle 3、7、10、14、17、21、58、59、60、61、62、63 increased remarkably after soil arching was formed, while, the stress measured by measurement circle 4、5、6、11、12、13、18、19、20、25、26、27 decreased remarkably after soil arching was formed, by which the soil arching formed could be determined (Depicted as a dashed line in Figure 10). The lower bound of soil arching was a circular arch which radius was 40mm and the upper bound was an elliptic arch which long axis was 190mm and short axis 100mm. The shape of soil arching is very similar to that of acquired by model test.

3.2.2 Dynamic Stresses

When the loads were $0.6+0.3\sin 20\pi t$ (KN), the soil arch collapse and when the loads were $0.6+0.2\sin 20\pi t$ (KN) and $0.6+0.1\sin 20\pi t$ (KN), the soil arching did not collapse throughout the entire computing process. It could be considered that there might be a critical dynamic load for the soil arching. When dynamic loads were less than the critical load, soil arching will not be failure. By contrast, soil arching will collapse. After dynamic load applied on, if soil arching did not collapse, dynamic stress increase at first and then will remain at a stable value. If soil arching collapse, after increasing to a maximum value, the dynamic stress decrease sharply. As showed in Figure 11. The result was similar to that of required by model test.

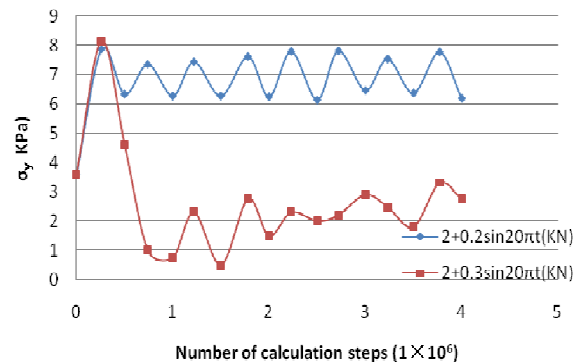
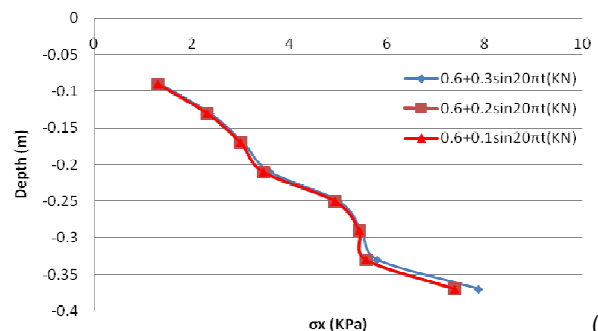


Figure 11. Stress versus number of calculation steps



(a)

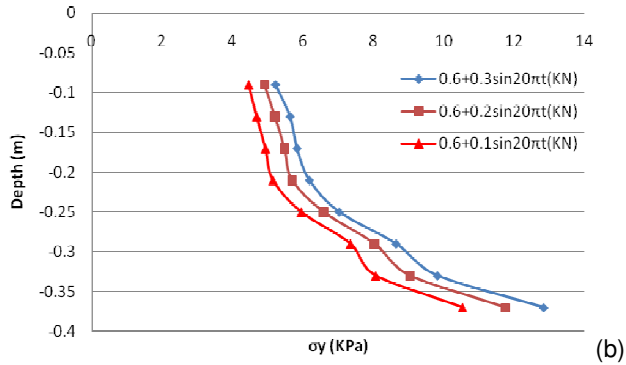


Figure 12. Stress along line A

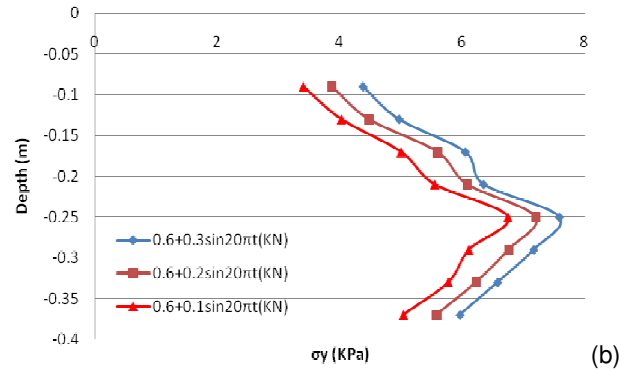


Figure 14. Stress along line C

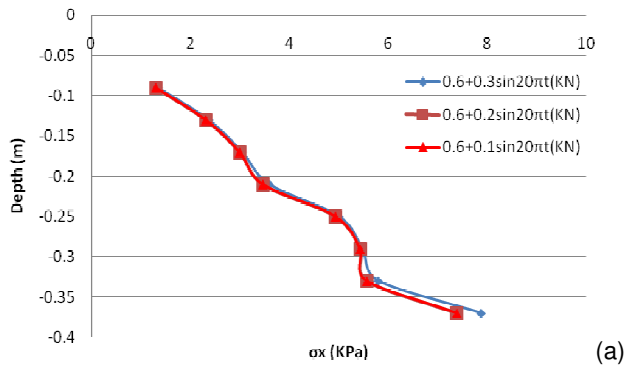


Figure 13. Stress along line B

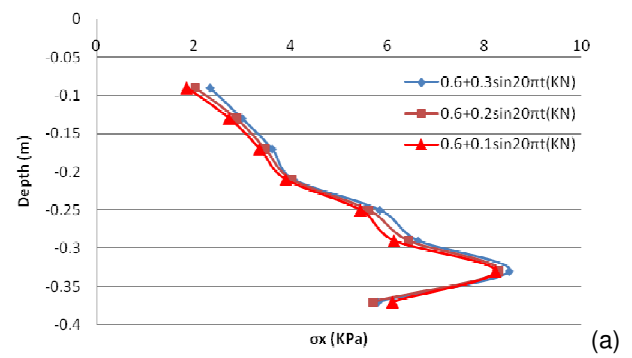
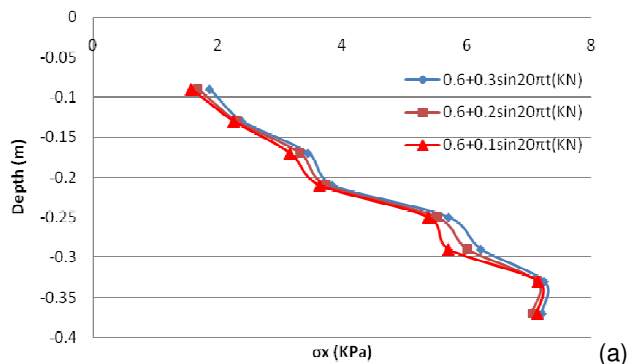
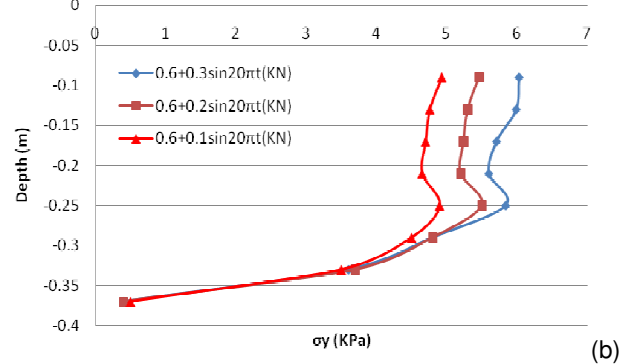
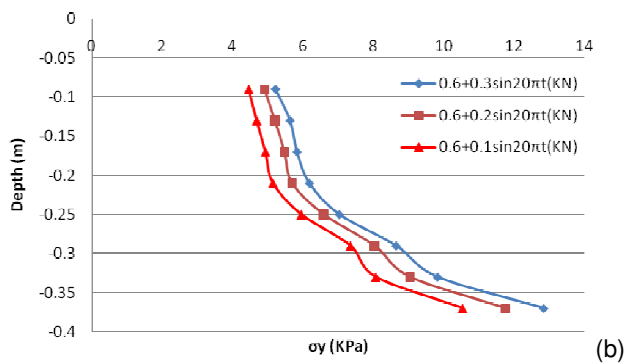


Figure 15. Stress along line D



When there is a soil arching, both horizontal and vertical stress have a mutation in soil. Both the horizontal and vertical stress will increase at both sides of soil and decrease in the center of soil (As showed in Figure 12-15, the location of A、B、C、D showed in Figure 10). It denotes that there is dynamic stress transfer in soil because of the existence of soil arching.

4 CONCLUSIONS

The results show that there is also transfer for the stress induced by external dynamic load because of soil arching. The thickness of the covering soil and the amplitude of the dynamic loads have an influence on the soil arching under dynamic load. With an increase in thickness of the covering soil, the required time of failure of soil arching increased significantly, however, with

increase of the amplitude of dynamic loads, the possibility of failure of soil arch also increase. Due to the soil arching the dynamic stress transfer in soil.

ACKNOWLEDGEMENT

The study was supported by the Key Research Project of Ministry of Railway, China (Project No. 2010G003-A) and is greatly appreciated.

REFERENCE

- C. Yun-min, C. Wei-ping, C. Ren-peng (2008). "An experimental investigation of soil arching within basal reinforced and unreinforced piles embankments." *Geotext. Geomembr.* 26 (2) 164 - 174.
- Hewlett, W.J., Randolph, M.F. (1988). "Analysis of piled embankments." *Ground Engineering*, 21 (3), 12 - 18.
- Itasca, Itasca Consulting Group (2004). *Particle Flow Code in Two Dimensions.*, Inc., Minnesota.
- J. Han, M.A. Gabr (2002). "Numerical analysis of geosynthetic-reinforced and pile-supported earth platform over soft soil." *J. Geotech. Environ. Eng. (ASCE)* 128(1) 44 - 53.
- Low, B.K., Tang, S.K., Choa, V. (1994). "Arching in piled embankments." *ASCE Journal of Geotechnical Engineering* 120 (11), 1917 - 1938.
- O. Jenck, D. Dias, R. Kastner (2007). "Two-dimensional physical and numerical modeling of a pile-supported earth platform over soft soil." *J. Geotech. Environ. Eng. (ASCE)* 133 (3) 295 - 305.
- Terzaghi, K. (1943). "Theoretical Soil Mechanics." Wiley, New York.